Published in final edited form as:
Mol Genet Genomics. 2010 April ; 283(4): 341–349. doi:10.1007/s00438-010-0522-y.

High-throughput assessment of CpG site methylation for distinguishing between HCV-cirrhosis and HCV-associated hepatocellular carcinoma

Kellie J. Archer,
Department of Biostatistics, Virginia Commonwealth University, 730 East Broad Street, P.O. Box 980032, Richmond, VA 23298-0032, USA. kjarcher@vcu.edu

Department of Surgery, Division of Transplantation, Virginia Commonwealth University, Richmond, VA 23298, USA

Valeria R. Mas,
Department of Surgery, Division of Transplantation, Virginia Commonwealth University, Richmond, VA 23298, USA

Department of Pathology, Virginia Commonwealth University, Richmond, VA 23298, USA

Daniel G. Maluf, and
Department of Surgery, Division of Transplantation, Virginia Commonwealth University, Richmond, VA 23298, USA

Robert A. Fisher
Department of Surgery, Division of Transplantation, Virginia Commonwealth University, Richmond, VA 23298, USA

Abstract

Methylation of promoter CpG islands has been associated with gene silencing and demonstrated to lead to chromosomal instability. Therefore, some postulate that aberrantly methylated CpG regions may be important bio-markers indicative of cancer development. In this study we used the Illumina GoldenGate Methylation BeadArray Cancer Panel I for simultaneously profiling methylation of 1,505 CpG sites in order to identify methylation differences in 76 liver tissues ranging from normal to pre-neoplastic and neoplastic states. CpG sites for *ESR1, GSTM2*, and *MME* were significantly differentially methylated when comparing the pre-neoplastic tissues from patients with concomitant hepatocellular carcinoma (HCC) to the pre-neoplastic tissues from patients without HCC. When comparing paired HCC tissues to their corresponding pre-neoplastic non-tumorous tissues, eight CpG sites, including one CpG site that was hypermethylated (*APC*) and seven (*NOTCH4, EMR3, HDAC9, DCL1, HLA-DOA, HLA-DPA1*, and *ERN1*) that were hypomethylated in HCC, were identified. Our study demonstrates that high-throughput methylation technologies may be used to identify differentially methylated CpG sites that may prove to be important molecular events involved in carcinogenesis.

Correspondence to: Kellie J. Archer.

Communicated by S. Hohmann.

Electronic supplementary material The online version of this article (doi:10.1007/s00438-010-0522-y) contains supplementary material, which is available to authorized users.

Keywords

Liver neoplasms; Gene silencing; Epigenesis genetic; Gene expression; Gene expression profiling

Introduction

High-throughput genomic technologies are increasingly being used in science and industry to identify therapeutic targets and risk-factors for specific diseases. As some notable examples, gene expression microarrays have been successfully used in differentiating two types of leukemia (Golub et al. 1999), and as prognostic meta-signatures for breast cancer (van't Veer et al. 2002, 2003; van de Vijver et al. 2002), lung adenocarcinoma (Beer et al. 2002), and diffuse large B-cell lymphoma (Rosenwald et al. 2002). As in other disease areas, through use of high-throughput technologies, a vast amount of information is being accumulated for the study of hepatocellular carcinoma (HCC). To date, most high-throughput genomic research in HCC has emphasized gene expression levels (Iizuka et al. 2004; Mas et al. 2006; Nam et al. 2005). However, the importance of epigenetic events is being elucidated, as aberrant methylation has been reported to lead to chromosomal instability (Baylin et al. 2000, 2001). In fact, methylation has been demonstrated to lead to genetic damage in colorectal tumors (Jones and Laird 1999). It has therefore been postulated that genomic aberrations may result from epigenetic events rather than being the causal events which lead to the development of cancer (Baylin et al. 2000, 2001). Moreover, aberrant methylation may directly affect gene expression by interfering with transcription factors. Unfortunately, the contribution of DNA methylation to the molecular pathogenesis of HCC is not well understood. Since methylation sensitive polymerase chain reaction (MSP) has been used in most studies examining methylation in HCC, most studies have examined a single or a limited number of genes (Jicai et al. 2006; Kondo et al. 2000; Qiu et al. 2007; Wong et al. 1999, 2000a, b). We postulated that methylation may play an important role in the pathogenesis of HCC, and that high-throughput screening of CpG sites may readily identify methylation events important in hepatocarcinogenesis.

Two previously published studies used high-throughput technologies for studying DNA methylation in HCC patients. In an early study that used restriction landmark genomic scans, investigators examined ~1,200 spots and identified the number of spots that changed between HCC and non-cancerous liver samples, concluding that the number of spots that changed was of prognostic importance (Itano et al. 2000). However, they did not clone any of the eight spots reported to be consistently changing in the HCC samples. In a more recent study that used methylated CpG island amplification microarrays (MCAM), researchers examined 6,458 CpG islands and identified 719 hypermethylated CpG islands (Gao et al. 2008). However, in this study only 10 HCC patients samples were examined using MCAM and significant CpG islands were determined by a fold-change threshold rather than statistical significance. As the cirrhotic liver has been described as being pre-malignant or a preneoplastic condition (McCaughan et al. 2002), herein we studied a set of homogeneous samples having a common underlying etiology of cirrhosis due to HCV infection, and used the Illumina GoldenGate Methylation BeadArray Cancer Panel I for simultaneously profiling methylation of 1,505 CpG sites in 76 liver tissues representing the progression to hepatocellular carcinoma combined with inferential testing to identify methylation events important in hepatocarcinogenesis.

Materials and methods

Patients and samples

Liver tissue from 20 HCV-HCC tumors and their adjacent non-tumorous HCV-cirrhotic tissues as well as 16 independent HCV-cirrhotic tissues from patients without concomitant HCC were

procured from patients undergoing liver transplantation. The Institutional Review Board approved the study protocol at Virginia Commonwealth University and written informed consent for procuring the tissue samples was obtained from all patients. In addition, 20 normal liver tissues were procured. Characteristics of the included study subjects are reported in Table 1. Since global hypomethylation and promoter-specific hypermethylation have been implicated in the process of aging, we selected this subset of 20 normal liver tissues from among the set of available normal donor livers as having age ≥40 years, to closely match the age distribution of the HCV-cirrhosis and HCV-HCC patients included.

Illumina GoldenGate Methylation BeadArray

DNA was isolated using QIA amp DNA Mini Kit (Qiagen) according to the manufacturer's instructions. The EZ DNA methylation kit (Zymo Research) was used for bisulfite conversion of all DNA (1 μg) samples. Universal Methylated DNA standard (Zymo Research) was included in duplicate in the plate (methylated and bisulfite treated). After bisulfite treatment, the remaining procedures were identical to the GoldenGate genotyping assay (Fan et al. 2003), using Illumina-supplied reagents and conditions. Specifically, in this study the GoldenGate Methylation Cancer Panel I was used as the methylation assay. For each CpG site, two pairs of probes are required: an allele-specific and locus-specific oligo designed to match the methylated target sequence and an allele-specific and locus-specific oligo designed to match unmethylated target sequence. After extension and ligation, the ligated products were amplified using universal primers and hybridized to an Illumina 96-sample Universal Array Matrix (SAM) for interrogating CpG sites. The array hybridization was conducted under a temperature gradient and the arrays were imaged using a BeadArray Reader. To assess performance of the system, DNA from 12 samples (6 paired HCV-HCC and adjacent HCV-cirrhotic samples) underwent bisulfite conversion procedure independently and were hybridized. Two controls were hybridized in duplicate; the duplicate controls were aliquots from the same tube post-bisulfite conversion.

Evaluation of methylation using MethyLight reactions

For validating the Illumina results for selected genes (*APC, GSTP1, PITX2*, and *ERBB2*), a set of samples hybridized to Illumina Universal Array Matrix were also evaluated using MethyLight (Eads et al. 2000; Trinh et al. 2001). Seventeen liver tissue samples, including two normal livers, five HCV-cirrhotic tissues, and five paired HCV HCC tumor and adjacent non-tumorous HCV-cirrhotic liver tissues studied using Illumina were included in the validation study. Methylation-specific TaqMan probes and specific primers were used in the reaction for each of the four genes. EpiTect Methylight Assays (Hs_ERBB2 and Hs_PITX2) (Qiagen, Valencia, CA) were used with EpiTect Methylight PCR kit. In addition, primers and probes were synthesized for *APC* and *GSTP1* (Applied Biosystems). These dual-labeled probes were methylation-specific oligonucleotides with a fluorophore (FAM or VIC) and a quencher moiety attached (TAMRA). After sodium bisulfite conversion, genomic DNA was amplified (Initial activation: 5 min 95°C, 15 s 95°C, 60 s 60°C for 45 cycles) and the fluorescence was detected by the laser detector of the ABI 7700 Sequence Detection System (Perkin Elmer, Foster City,CA). A no template control, a fully methylated genomic DNA (EpiTect Control DNA methylated, Qiagen, Valencia, CA) and an unmethylated DNA (EpiTect Control DNA unmethlyated, Qiagen, Valencia, CA) were used as controls in each plate.

Statistical methods

Each CpG site is represented by a specific beadtype, and the assay incorporates ~30 beads per beadtype such that the redundancy enhances the assay's reproducibility. For each array *i* and CpG site (or beadtype) *j*, beadtype expression for the red (methylated) and green (unmethylated) channels was estimated by averaging the intensities over the beads within the

beadtype, yielding R_{ij} and G_{ij}. Background was estimated separately for the methylated and unmethylated states as the average intensity of the negative control beads for the red (Rb_i) and green channels (Gb_i), respectively, and was then subtracted from the beadtype intensities on array i. Thereafter, a summary statistic representing "percent methylated" was estimated as the methylated signal (M_{ij}) divided by the sum of the methylated (M_{ij}) and unmethylated (U_{ij}) signals after background adjustment, symbolically

$$\beta_{ij}=\frac{\max(R_{ij}-Rb_i,0)}{\max(R_{ij}-Rb_i,0)+\max(G_{ij}-Gb_i,0)}=\frac{M_{ij}}{M_{ij}+U_{ij}},$$

where the maximum of the background corrected intensity and 0 was taken to avoid calculation of negative percent methylated values. Data processing was performed using the beadarray package (Dunning et al. 2007) in the R programming environment (R Core Development Team 2007). These data have been made publicly available in NCBI's Gene Expression Omnibus (Barrett et al. 2005; Edgar et al. 2002) and are accessible through GEO Series accession number GSE18081 (http://www.ncbi.nlm.nih.gov/geo/query/acc.cgi?acc=GSE18081).

For each CpG site, the paired HCV-HCC and adjacent HCV-cirrhotic tissues were compared with respect to percent methylated using a paired *t*-test. In addition, a Jonckheere-Terpstra test was applied to identify whether there was a significant monotonic trend in percent methylation across the independent normal, HCV-cirrhotic, and HCV-HCC tissues. In other words, for testing whether there was a significant increasing monotonic trend the null hypothesis tested was H_0: $\beta_{\text{Normal}} \leq \beta_{\text{HCV-cirrhosis}} \leq \beta_{\text{HCV-HCC}}$ against the alternative that one of the inequalities was strict. Similarly, for testing whether there was a significant decreasing monotonic trend the null hypothesis tested was H_0: $\beta_{\text{Normal}} \geq \beta_{\text{HCV-cirrhosis}} \geq \beta_{\text{HCV-HCC}}$ against the alternative that one of the inequalities was strict. When comparing the HCV-cirrhotic tissues from patients without concomitant HCC to HCV-cirrhotic tissues from patients with HCC, a two-sample *t*-test was used. The resulting *P*-values were used in estimating false discovery rates (FDR) using the *Q*-value method (Storey and Tibshirani 2003); CpG sites with an FDR < 0.10 were considered significant.

For the MethyLight reactions, calculations of the methylation rate were calculated as:

$$\text{Percentage of methylation:Cmeth}=100/\left[1+2^{(\text{CtCG}-\text{Ct TG})}\right]\%$$

where Ct CG (FAM) represents the threshold cycle of the CG reporter (FAM channel), and Ct TG (VIC) represents the threshold cycle of the TG reporter (VIC channel). Samples were evaluated in duplicate and the Ct mean values were used for the final calculation. Pearson's correlation coefficient (ρ) was calculated to examine the relation between Illumina and MethyLight results and genes with a *P*-value <0.05 were considered significant.

Results

CpG sites differentially methylated between HCV-cirrhotic tissues from patients with and without HCC

We first investigated whether cirrhotic tissues from HCV-infected patients with and without HCC differed with respect to methylation. Statistically, 21 CpG sites were significantly differentially methylated when comparing the non-tumorous HCV-cirrhotic tissues from patients with HCV-HCC to the cirrhotic tissues from patients with HCV-cirrhosis without HCC. For each CpG site identified, its distance from the transcription start site (TSS) and whether a CpG island is present in the gene promoter region are provided. It has been

demonstrated that transcription binding sites are largely within nucleosome-free regions (NFR) (Li et al. 2007). Although for this platform CpG site positioning relative to nucleosomes is not known, one could infer that NFR are predominantly 200 bp upstream of the TSS (Gao et al. 2008; Yuan et al. 2005). For these 21 CpG sites, the median distance from the TSS was −135. Genes with significant differential CpG site methylation between HCV-cirrhosis with and without concomitant HCC with an absolute difference between proportion methylated of at least 0.17 were *ESR1*, *GSTM2*, and *MME* (Table 2). The difference threshold of 0.17 was based on a previous publication in which a maximum standard deviation of 0.06 was observed among technical replicates for 18 gender-specific CpG sites in a mixture study of male and female genomic DNA (Bibikova et al. 2006b). A representative boxplot of percent methylated for *ESR1* demonstrates the increasing methylation pattern in cirrhosis with concomitant HCC compared to cirrhosis without concomintant HCC (Fig. 1). The *ESR1* gene has been associated with a variety of cancers and apart from its role in the estrogen receptor signaling pathway transcription, it has been found to play a role in the regulation of transcription. The *GSTM2* gene encodes a glutathione *S*-transferase that is involved in electrophilic compound detoxification. *MME* is implicated in cancer, particularly leukemia, and its biological functions include proteolysis and cell-cell signaling.

The 21 significant genes were subsequently used in performing pathway analyses using the Ingenuity Pathways Analysis software (Ingenuity® Systems, Release Number 7.1, www.ingenuity.com). The associated molecular and cellular functions were cellular development (*ALK, BMP4, BMP6, ESR1, HOXB13, ITK, MYB, NOTCH4, PGF, SMAD2, TGFB2*; *P*-value range = 0.00000311–0.0132) and cellular growth and proliferation (includes the previous list and additionally, *FRK* and *TMEFF2*; *P*-value range = 0.00000702–0.0132). The top three canonical pathways were factors promoting carcinogenesis in vertebrates ($P = 0.00000835$), Transforming growth factor beta (*TGF-β*) signaling ($P = 0.000293$), and hepatic fibrosis/hepatic stellate cell activation ($P = 0.00111$). The *TGF*-β signaling pathway is involved in a number of cellular processes including cellular growth, differentiation, and apoptosis. Hepatic stellate cell activation leads to the development of hepatic fibrosis, which in patients included in this study, is likely triggered by the inflammatory response due to HCV infection. Severe fibrosis leads to cirrhosis of the liver, which has been described as a pre-malignant or a preneoplastic condition (McCaughan et al. 2002).

CpG sites differentially methylated comparing paired HCV-HCC and adjacent HCV-cirrhotic non-tumorous liver tissues

When statistically comparing paired HCV-HCC and adjacent HCV-cirrhotic non-tumorous liver tissue samples, 56 CpG sites (corresponding to 49 unique genes) were identified as differentially methylated. For these 56 CpG sites, the median distance from the TSS was −190. Among these, eight CpG sites exhibited an absolute difference in proportion methylated > 0.17 (Table 2). This included one CpG site that was hypermethylated in HCC tissues compared to the corresponding non-tumorous cirrhotic tissues (*APC*). The remaining seven (*NOTCH4, EMR3, HDAC9, DCL1, HLA-DOA, HLA-DPA1*, and *ERN1*) were hypomethylated in HCC (Table 3).

CpG sites with significant monotonic trend in proportion methylated among normal, HCV-cirrhosis, and HCV-HCC

235 CpG sites had a significant increasing trend in proportion methylated, with a median distance from the TSS of −221 (hypermethylated), while 266 CpG sites had a significant decreasing trend, with a median distance from the TSS of −188 (hypomethylated), as tissue progressed from normal, to cirrhosis, to HCC (FDR < 5% each comparison, for total FDR < 10%). For 50 of the 235 significant CpG sites with a significant increasing trend, the difference in proportion methylated between HCV-HCC and normal exceeded the established threshold

of 0.17 (Supplemental Table 1). Among these 50 some genes are listed more than once because for some genes the assay interrogates more than one CpG site. CpG sites with significant hypermethylation were located in the promoter regions of genes known to be important in carcinogenesis, included genes associated with other cancers such as *ACVR1, ALOX12, COL1A1, DDIT3 FLT3, HOXA5, HOXA9*, and *MMP14* among others. For 94 of the 266 significant CpG sites with a significant decreasing trend, the absolute value of the difference in proportion methylated between HCV-HCC and normal exceeded the established threshold of 0.17 (Supplemental Table 2). *BMP4*, *ESR1*, *GSTP1*, *HDAC1*, *PDGFRB*, and *RASSF1* were among the CpG sites having a significant decreasing trend and reduced or lost expression of these genes has been noted in other cancers. Based on the Ingenuity Pathways analysis, the top canonical pathway for the CpG sites exhibiting a significant increasing trend was Hepatic Fibrosis/Hepatic Stellate Activation (P = 6.17E-08).

Correlation between Illumina GoldenGate Methylation BeadArray Cancer Panel I and MethyLight

Although the Illumina assay has been rigorously tested (Bibikova et al. 2006a, b), we examined the concordance of our high-throughput Illumina results using a more sensitive assay, MethyLight for CpGs associated with some selected genes. We found that the proportion methylated obtained from the Illumina methylation assay was significantly correlated with the MethyLight results for *APC1, ERBB2, GSTP1*, and *PITX2* ($\rho = 0.90$, $P < 0.0001$; $\rho = 0.71$, $P = 0.001$; $\rho = 0.58$, $P = 0.02$; and $\rho = 0.52$, $P = 0.03$, respectively).

Comparison with previous findings

In a recent study that used methylated CpG island amplification microarrays (MCAM), researchers examined 6,458 CpG islands and identified 719 hypermethylated CpG islands (Gao et al. 2008). However, in this study only 10 HCC patients samples were examined using MCAM and significant CpG islands were determined by a fold-change threshold rather than statistical significance. Nevertheless, when merging these 719 CpG islands by gene symbol to CpG sites identified as statistically significant in the previous analyses, we identified that 43 CpG sites for 32 unique genes were in common between the two studies (Table 4).

Discussion

Using a high-throughput platform, in this study we identified several CpG sites that were differentially methylated among liver tissues representing the progression from normal, to HCV-cirrrhosis, to HCV-HCC. From our analyses, we found the reproducibility of the Illumina GoldenGate Methylation assay to be very high even for samples that independently underwent bisulfite conversion. We also used MethyLight reactions for validating selected genes identified from the analyses using the Illumina GoldenGate Methylation assay. The MethyLight assay is reproducible and sensitive and its correlation with the Illumina GoldenGate Methylation assay demonstrates we can reliably detect methylation in DNA samples using this high-throughput technology.

Our study design was restricted to subjects having the same underlying cirrhosis etiology, as it has been noted that patients with HBV-HCC likely have different malignant transforming mechanisms compared to patients with HCV-HCC (Iizuka et al. 2004; Moinzadeh et al. 2005; Poon et al. 2006). In fact, the difference between HCV and HBV etiologies was emphasized in two recent methylation studies. In the first, researchers examined methylation of 19 epigenetic markers in 77 paired HCC and matching non-cancerous liver tissue along with 22 normal liver tissues (Nishida et al. 2008). The authors found that 7/19 epigenetic markers (*COX2, MINT1, CACNA1G, RASSF2, MINT2, Reprimo*, and *DCC*) were hypermethylated in HCV+ tissues in comparison to both HBV+ and normal liver tissues. The authors concluded

that HCV infection may accelerate the methylation process. In the second, investigators examined 24 different gene promoter regions using MSP in conjunction with DNA sequencing in 28 HBV/HCC tissues and corresponding non-tumorous tissues (Yu et al. 2003) and found that 15 of the 24 were more frequently methylated among HCC versus HCV tissues. This suggests that monitoring important epigenetic markers may be of clinical utility but that different markers would be needed for HCV and HBV. We believe our study design, which, similar to previously published gene expression and microarray studies (Llovet et al. 2006; Wurmbach et al. 2007), is restricted to patients with a common etiology of HCV infection, is better able to identify molecular events involved in the disease process. Developing an appropriate study design is of vital importance when identifying molecular events in carcinogenesis.

A limitation to our study was the small sample size available for each of tissue type (normal ($N = 20$), cirrhosis without HCC ($N = 16$), cirrhosis with concomitant HCC ($N = 20$), and HCC ($N = 20$)). However, we were able to corroborate some previous findings. For example, we identified the *APC* gene to be hypermethylated in HCC tissues compared to adjacent non-tumorous cirrhotic tissues. Other investigators previously found that the APC promoter was hypermethylated in 81.8% of non-cancerous liver tissue samples (Csepregi et al. 2008). In that study all HCC studied samples and ten patients with liver metastasis (52.6%) exhibited APC promoter methylation. The degree of methylation was significantly higher in samples from HCC compared to the non-cancerous liver tissue samples (63.1 vs. 24.98%; $P = 0.001$). Moreover, the level of APC protein expression was significantly reduced in HCC samples compared to that of the corresponding non-tumor liver tissue ($P < 0.05$). These results suggest that promoter methylation of the *APC* gene is important in hepatocarcinogenesis, and its hypermethylation results in reduced protein expression in HCC. Interestingly, the APC gene encodes a tumor suppressor protein that has been extensively studied in colon cancer. Though HCC surveillance has been demonstrated to lead to early HCC detection which in turn reduces the percent of untreated patients with disease (Trevisani et al. 2007), due to the poor sensitivities and specificities of currently used biomarkers, namely AFP and PIVKA-II (Beale et al. 2008, Ishii et al. 2000, Sherman 2007), additional markers that are more sensitive and specific for early HCC detection are needed. We conclude that larger high-throughput DNA methylation studies may reveal important methylation events, such as APC, that may serve as novel biomarkers for HCC screening.

Supplementary Material

Refer to Web version on PubMed Central for supplementary material.

Acknowledgments

This project was supported by a National Institute of Diabetes and Digestive and Kidney Diseases (NIDDK) grant, RO1DK069859.

References

Barrett T, Suzek TO, Troup DB, Wilhite SE, Ngau WC, Ledoux P, Rudnev D, Lash AE, Fujibuchi W, Edgar R. NCBI GEO: mining millions of expression profiles—database and tools. Nucleic Acids Res 2005;33:D562–D566. [PubMed: 15608262]

Baylin SB, Belinsky SA, Herman JG. Aberrant methylation of gene promoters in cancer—concepts, misconcepts, and promise. J Natl Cancer Inst 2000;92:1460–1461. [PubMed: 10995795]

Baylin SB, Esteller M, Roundtree MR, Bachman KE, Schuebel K, Herman JG. Aberrant patterns of DNA methylation, chromatin formation and gene expression in cancer. Hum Mol Genet 2001;10:687–692. [PubMed: 11257100]

Beale G, Chattopadhyay D, Gray J, Stewart S, Hudson M, Day C, Trerotoli P, Giannelli G, Manas D, Reeves H. AFP, PIVKAII, GP3, SCCA-1 and follisatin as surveillance biomarkers for hepatocellular cancer in non-alcoholic and alcoholic fatty liver disease. BMC Cancer 2008;8:200. [PubMed: 18638391]

Beer DG, Kardia SL, Huang CC, Giordano TJ, Levin AM, Misek DE, Lin L, Chen G, Gharib TG, Thomas DG, Lizyness ML, Kuick R, Hayasaka S, Taylor JM, Iannettoni MD, Orringer MB, Hanash S. Gene-expression profiles predict survival of patients with lung adenocarcinoma. Nat Med 2002;8:816–824. [PubMed: 12118244]

Bibikova M, Chudin E, Wu B, Zhou L, Garcia EW, Liu Y, Shin S, Plaia TW, Auerbach JM, Arking DE, Gonzalez R, Crook J, Davidson B, Schulz TC, Robins A, Khanna A, Sartipy P, Hyllner J, Vanguri P, Savant-Bhonsale S, Smith AK, Chakravarti A, Maitra A, Rao M, Barker DL, Loring JF, Fan J-B. Human embryonic stem cells have a unique epigenetic signature. Genome Res 2006a;16:1075–1083. [PubMed: 16899657]

Bibikova M, Lin Z, Zhou L, Chudin E, Garcia EW, Wu B, Doucet D, Thomas NJ, Wang Y, Vollmer E, Goldmann T, Seifart C, Jiang W, Barker DL, Chee MS, Floros J, Fan J-B. High-throughput DNA methylation profiling using universal bead arrays. Genome Res 2006b;16:383–393. [PubMed: 16449502]

But DY, Lai CL, Yuen MF. Natural history of hepatitis-related hepatocellular carcinoma. World J Gastroenterol 2008;14:1652–1656. [PubMed: 18350595]

Calvisi DF, Ladu S, Gorden A, Farina M, Lee JS, Conner EA, Schroeder I, Factor VM, Thorgeirsson SS. Mechanistic and prognostic significance of aberrant methylation in the molecular pathogenesis of human hepatocellular carcinoma. J Clin Invest 2007;117:2713–2722. [PubMed: 17717605]

Csepregi A, Rocken C, Hoffmann J, Gu P, Saliger S, Muller O, Schneider-Stock R, Kutzner N, Roessner A, Malfertheiner P, Ebert MP. APC promoter methylation and protein expression in hepatocellular carcinoma. J Cancer Res Clin Oncol 2008;134:579–589. [PubMed: 17973119]

Dunning MJ, Smith ML, Ritchie ME, Tavare S. beadarray: R classes and methods for Illumina bead-based data. Bioinformatics 2007;23:2183–2184. [PubMed: 17586828]

Eads CA, Danenberg KD, Kawakami K, Saltz LB, Blake C, Shibata D, Danenberg PV, Laird PW. MethyLight: a high-throughput assay to measure DNA methylation. Nucleic Acids Res 2000;28:E32. [PubMed: 10734209]

Edgar R, Domrachev M, Lash AE. Gene Expression Omnibus: NCBI gene expression and hybridization array data repository. Nucleic Acids Res 2002;30:207–210. [PubMed: 11752295]

Fan JB, Oliphant A, Shen R, Kermani BG, Garcia F, Gunderson KL, Hansen M, Steemers F, Butler SL, Deloukas P, Galver L, Hunt S, McBride C, Bibikova M, Rubano T, Chen J, Wickham E, Doucet D, Chang W, Campbell D, Zhang B, Kruglyak S, Bentley D, Haas J, Rigault P, Zhou L, Stuelpnagel J, Chee MS. Highly parallel SNP genotyping. Cold Spring Harb Symp Quant Biol 2003;68:69–78. [PubMed: 15338605]

Fox BP, Tabone CJ, Kandpal RP. Potential clinical relevance of Eph receptors and ephrin ligands expressed in prostate carcinoma cell lines. Biochem Biophys Res Commun 2006;342:1263–1272. [PubMed: 16516143]

Gao W, Kondo Y, Shen L, Shimizu Y, Sano T, Yamao K, Natsume A, Goto Y, Ito M, Murakami H, Osada H, Zhang J, Issa JP, Sekido Y. Variable DNA methylation patterns associated with progression of disease in hepatocellular carcinomas. Carcinogenesis 2008;29:1901–1910. [PubMed: 18632756]

Golub TR, Slonim DK, Tamayo P, Huard C, Gaasenbeek M, Mesirov JP, Coller H, Loh ML, Downing JR, Caligiuri MA, Bloomfield CD, Lander ES. Molecular classification of cancer: class discovery and class prediction by gene expression monitoring. Science 1999;286:531–537. [PubMed: 10521349]

Iizuka N, Hamamoto Y, Oka M. Predicting individual outcomes in hepatocellular carcinoma. Lancet 2004;364:1837–1839. [PubMed: 15555651]

Itano O, Ueda M, Kikuchi K, Shimazu M, Kitagawa Y, Aiura K, Kitajima M. A new predictive factor for hepatocellular carcinoma based on two-dimensional electrophoresis of genomic DNA. Oncogene 2000;19:1676–1683. [PubMed: 10763824]

Jicai Z, Zongtao Y, Jun L, Haiping L, Jianmin W, Lihua H. Persistent infection of hepatitis B virus is involved in high rate of p16 methylation in hepatocellular carcinoma. Mol Carcinog 2006;45:530–536. [PubMed: 16649250]

Jones PA, Laird PW. Cancer epigenetics comes of age. Nat Genet 1999;21:163–167. [PubMed: 9988266]

Kondo Y, Kanai Y, Sakamoto M, Mizokami M, Ueda R, Hirohashi S. Genetic instability and aberrant DNA methylation in chronic hepatitis and cirrhosis—a comprehensive study of loss of heterozygosity and microsatellite instability at 39 loci and DNA hypermethylation on 8 CpG islands in microdissected specimens from patients with hepatocellular carcinoma. Hepatology 2000;32:970–979. [PubMed: 11050047]

Li B, Carey M, Workman JL. The role of chromatin during transcription. Cell 2007;128:707–719. [PubMed: 17320508]

Llovet JM, Chen Y, Wurmbach E, Roayaie S, Fiel MI, Schwartz M, Thung SN, Khitrov G, Zhang W, Villanueva A, Battiston C, Mazzaferro V, Bruix J, Waxman S, Friedman SL. A molecular signature to discriminate dysplastic nodules from early hepatocellular carcinoma in HCV cirrhosis. Gastroenterology 2006;131:1758–1767. [PubMed: 17087938]

Mas VR, Maluf DG, Archer KJ, Yanek K, Williams B, Fisher RA. Differentially expressed genes between early and advanced hepatocellular carcinoma (HCC) as a potential tool for selecting liver transplant recipients. Mol Med 2006;12:97–104. [PubMed: 16953559]

McCaughan GW, Koorey DJ, Strasser SI. Hepatocellular carcinoma: current approaches to diagnosis and management. Intern Med J 2002;32:394–400. [PubMed: 12162396]

Moinzadeh P, Breuhahn K, Stutzer H, Schirmacher P. Chromosome alterations in human hepatocellular carcinomas correlate with aetiology and histological grade—results of an explorative CGH meta-analysis. Br J Cancer 2005;92:935–941. [PubMed: 15756261]

Nam SN, Park JY, Ramasamy A, Shevade S, Islam A, Long PM, Park CK, Park SE, Kim SY, Lee SH, Park WS, Yoo NJ, Liu ET, Miller LD, Lee JY. Molecular changes from dysplastic nodule to hepatocellular carcinoma through gene expression profiling. Hepatology 2005;42:809–818. [PubMed: 16175600]

Nishida N, Nagasaka T, Nishimura T, Ikai I, Boland CR, Goel A. Aberrant methylation of multiple tumor suppressor genes in aging liver, chronic hepatitis, and hepatocellular carcinoma. Hepatology 2008;47:908–918. [PubMed: 18161048]

Poon TCW, Wong N, Lai PBS, Rattray M, Johnson PJ, Sung JJY. A tumor progression model for hepatocellular carcinoma: bioinformatic analysis of genomic data. Gastroenterology 2006;131:1262–1270. [PubMed: 17030195]

Qiu GH, Xie H, Wheelhouse N, Harrison D, Chen GG, Salto-Tellez M, Lai P, Ross JA, Hooi SC. Differential expression of hDAB2IPA and hDAB2IPB in normal tissues and promoter methylation of hDAB2IPA in hepatocellular carcinoma. J Hepatol 2007;46:655–663. [PubMed: 17258345]

R Core Development Team. R: a language and environment for statistical computing. Vienna: R Foundation for Statistical Computing; 2007.

Rosenwald A, Wright G, Chan WC, Connors JM, Campo E, Fisher RI, Gascoyne RD, Muller-Hermelink HK, Smeland EB, Giltnane JM, Hurt EM, Zhao H, Averett L, Yang L, Wilson WH, Jaffe ES, Simon R, Klausner RD, Powell J, Duffey PL, Longo DL, Greiner TC, Weisenburger DD, Sanger WG, Dave BJ, Lynch JC, Vose J, Armitage JO, Montserrat E, Lopez-Guillermo A, Grogan TM, Miller TP, LeBlanc M, Ott G, Kvaloy S, Delabie J, Holte H, Krajci P, Stokke T, Staudt LM. The use of molecular profiling to predict survival after chemotherapy for diffuse large-B-cell lymphoma. N Engl J Med 2002;346:1937–1947. [PubMed: 12075054]

Sherman M. Surveillance for hepatocellular carcinoma and early diagnosis. Clin Liver Dis 2007;11:817–837. [PubMed: 17981230]

Storey JD, Tibshirani R. Statistical significance for genomewide studies. Proc Natl Acad Sci USA 2003;100:9440–9445. [PubMed: 12883005]

Trevisani F, Santi V, Gramenzi A, Di Nolfo MA, Del Poggio P, Benvegnu L, Rapaccini G, Farinati F, Zoli M, Borzio F, Giannini EG, Caturelli E, Bernardi M. Surveillance for early diagnosis of hepatocellular carcinoma: is it effective in intermediate/advanced cirrhosis? Am J Gastroenterol 2007;102:2448–2457. quiz 2458. [PubMed: 17617210]

Trinh BN, Long TI, Laird PW. DNA methylation analysis by MethyLight technology. Methods 2001;25:456–462. [PubMed: 11846615]

van de Vijver MJ, He YD, van't Veer LJ, Dai H, Hart AA, Voskuil DW, Schreiber GJ, Peterse JL, Roberts C, Marton MJ, Parrish M, Atsma D, Witteveen A, Glas A, Delahaye L, van der Velde T, Bartelink H, Rodenhuis S, Rutgers ET, Friend SH, Bernards R. A gene-expression signature as a predictor of survival in breast cancer. N Engl J Med 2002;347:1999–2009. [PubMed: 12490681]

van't Veer LJ, Dai H, van de Vijver MJ, He YD, Hart AA, Mao M, Peterse HL, van der Kooy K, Marton MJ, Witteveen AT, Schreiber GJ, Kerkhoven RM, Roberts C, Linsley PS, Bernards R, Friend SH. Gene expression profiling predicts clinical outcome of breast cancer. Nature 2002;415:530–536. [PubMed: 11823860]

van't Veer LJ, Dai H, van de Vijver MJ, He YD, Hart AA, Bernards R, Friend SH. Expression profiling predicts outcome in breast cancer. Breast Cancer Res 2003;5:57–58. [PubMed: 12559048]

Wong IHN, Lo YMD, Zhang J, Liew C-T, Ng MHL, Wong N, Lai PBS, Lau WY, Hjelm NM, Johnson PJ. Detection of aberrant p16 methylation in the plasma and serum of liver cancer patients. Cancer Res 1999;59:71–73. [PubMed: 9892188]

Wong IH, Lo YM, Lai PB, Johnson PJ. Relationship of p16 methylation status and serum alpha-fetoprotein concentration in hepatocellular carcinoma patients. Clin Chem 2000a;46:1420–1422. [PubMed: 10973879]

Wong IH, Lo YM, Yeo W, Lau WY, Johnson PJ. Frequent p15 promoter methylation in tumor and peripheral blood from hepatocellular carcinoma patients. Clin Cancer Res 2000b;6:3516–3521. [PubMed: 10999738]

Wurmbach E, Chen YB, Khitrov G, Zhang W, Roayaie S, Schwartz M, Fiel I, Thung S, Mazzaferro V, Bruix J, Bottinger E, Friedman S, Waxman S, Llovet JM. Genome-wide molecular profiles of HCV-induced dysplasia and hepatocellular carcinoma. Hepatology 2007;45:938–947. [PubMed: 17393520]

Yu J, Zhang HY, Ma ZZ, Lu W, Wang YF, Zhu JD. Methylation profiling of twenty-four genes and the concordant methylation behaviours of nineteen genes that may contribute to hepatocellular carcinogenesis. Cell Res 2003;13:319–333. [PubMed: 14672555]

Yuan GC, Liu YJ, Dion MF, Slack MD, Wu LF, Altschuler SJ, Rando OJ. Genome-scale identification of nucleosome positions in *Scerevisiae*. Science 2005;309:626–630. [PubMed: 15961632]

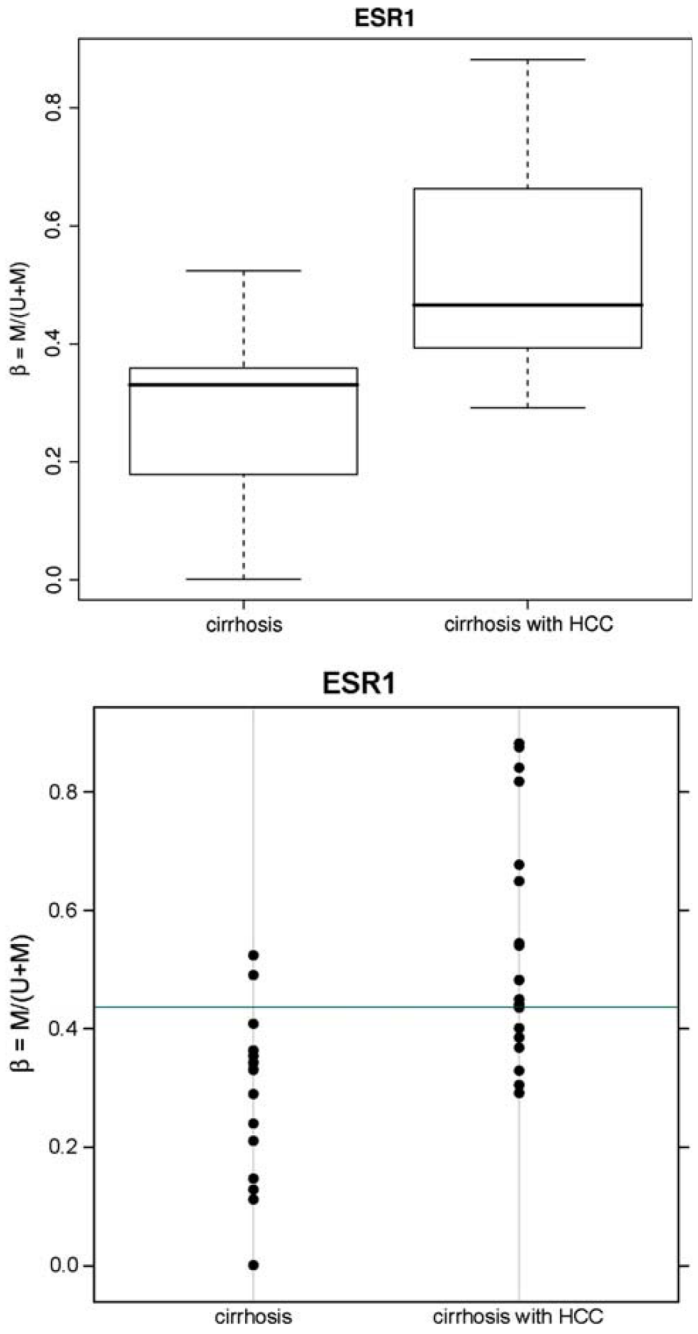

Fig. 1.

Illustrative boxplot and dotchart of percent methylated by tissue type (cirrhotic tissue from patients with concomitant HCC (cirrhosis with HCC) and cirrhotic tissues from patients without concomitant HCC (cirrhosis)) for *ESR1*

Table 1

Descriptive statistics consisting of mean ± SD for continuous variables and percent for categorical variables

	HCC with cirrhosis (*N* = 20)	**Cirrhosis without HCC (*N* = 16)**	**Normal (*N* = 20)**	***P*-value**
Age	53 (47, 66)	47 (30, 62)	59 (42, 73)	0.002
Gender (% male)	85	87.5	65	0.26
AFP	22.6 (3.0, 89.6)	6.8 (1.8, 130)		0.60
Albumin	2.8 (2.0, 3.9)	2.3 (1.7, 3.2)		0.008
WBC	4.3 (2.5, 13.5)	5.6 (3.2, 10.1)		0.55
HgB	12.2 (8.6, 14.7)	12.9 (8.0, 16.8)		0.53
PLT	62.5 (32.9, 139)	66 (9.5, 226)		0.54

Table 2

Genes associated with CpG sites differentially methylated when comparing the independent HCV-cirrhotic tissues from patients without concomitant HCC to HCV-cirrhotic tissues from patients with HCC

Gene symbol	Chromosome	Distance (bp) from transcriptional start site	CpG island in gene promoter region	*P*-value	*Q*-value	$\beta_{\text{HCV-cirrhosis with HCC}}$	$\beta_{\text{HCV-cirrhosis without HCC}}$	Difference
ESR1	6	−151	Y	0.00011	0.0465	0.532	0.289	0.243
GSTM2	1	153	Y	0.00040	0.0677	0.350	0.168	0.182
MME	3	−388	Y	0.00072	0.0783	0.284	0.109	0.175

Genes are sorted by the difference in proportion methylated between HCV-cirrhotic liver tissues with and without concomitant HCC

Table 3

Genes associated with CpG sites differentially methylated comparing paired HCV-HCC and adjacent HCV-cirrhotic non-tumorous tissues. Genes are sorted by the difference in proportion methylated between HCV-HCC and HCV-cirrhotic liver tissues

Gene symbol	Chromosome	Distance (bp) from transcriptional start site	CpG island in gene promoter region	*P*-value	*Q*-value	$\beta_{\text{HCV-HCC}} - \beta_{\text{HCV-cirrhosis}}$
APC	5	117	Y	0.0037	0.079	0.185
ERN1	17	−809	Y	0.0001	0.016	−0.173
HLA-DPA1	6	−28	N	0.0029	0.079	−0.176
HLA-DOA	6	−191	N	0.0035	0.079	−0.177
DLC1	8	276	N	0.0008	0.041	−0.194
HDAC9	7	−137	N	0.0000	0.012	−0.204
EMR3	19	61	N	0.0000	0.009	−0.257
NOTCH4	6	4	N	0.0002	0.024	−0.308

Table 4

CpG sites identified as statistically significant when comparing paired HCV-HCC and adjacent HCV-cirrhotic non-tumorous tissues (HCC vs adjacent), the independent HCV-cirrhotic tissues from patients without concomitant HCC to HCV-cirrhotic tissues from patients with HCC (Cirrhosis w/wo HCC), with a significant monotonic increasing trend (increasing trend), or with a significant monotonic decreasing trend (decreasing trend), that were also identified as significant in the Gao MCAM study

Symbol	Distance (bp) to transcription start site	CpG island in gene promoter region	*Q*-value	Gao cancer (R/G)	Gao adjacent (R/G)	Gao pattern	Illumina analysis
CD34	−780	N	0.079266	4.78	1.06	Cancer-specific pattern	HCC vs adjacent
SYK	−584	N	0.084625	8.27	1.11	Progression pattern	HCC vs adjacent
ABCA1	120	Y	0.046535	3.06	1.01	Cancer-specific pattern	Cirrhosis w/wo HCC
BMP6	−398	Y	0.085454	2.39	1.15	Progression pattern	Cirrhosis w/wo HCC
GABRB3	−92	Y	0.071951	3.36	1.38	Progression pattern	Cirrhosis w/wo HCC
HOXB13	−17	Y	0.046535	2.66	1.53	Progression pattern	Cirrhosis w/wo HCC
ALOX12	−223	Y	0.000198	7.69	2.11	Progression pattern	Increasing trend
ALOX12	85	Y	0.000931	7.69	2.11	Progression pattern	Increasing trend
ASCL2	−609	Y	0.002916	6.32	1.32	Progression pattern	Increasing trend
ASCL2	−360	Y	0.000239	6.32	1.32	Progression pattern	Increasing trend
CALCA	−75	Y	0.037769	4.24	0.97	Cancer-specific pattern	Increasing trend
CALCA	−171	Y	0.001417	4.24	0.97	Cancer-specific pattern	Increasing trend
CALCA	174	Y	0.043644	4.24	0.97	Cancer-specific pattern	Increasing trend
CRIP1	−874	Y	0.003467	2.29	1.07	Cancer-specific pattern	Increasing trend
CRIP1	−274	Y	0.002916	2.29	1.07	Cancer-specific pattern	Increasing trend
EPHA5	−66	Y	0.001028	2.08	1.15	Progression pattern	Increasing trend
ERBB2	−59	Y	0.03422	2.81	1.1	Progression pattern	Increasing trend
ERBB4	−255	Y	0.043644	14.31	2.38	Progression pattern	Increasing trend
EYA4	−794	Y	0.006918	4.85	1.1	Progression pattern	Increasing trend
FLT1	−615	Y	0.028504	4.49	1.16	Progression pattern	Increasing trend
FLT4	206	Y	0.047382	2.44	1.31	Progression pattern	Increasing trend
HHIP	−578	Y	0.047382	2.39	1.02	Cancer-specific pattern	Increasing trend
HOXA5	187	Y	<0.000001	2.03	1.74	Early pattern	Increasing trend
HOXA5	−479	Y	0.000736	2.03	1.74	Early pattern	Increasing trend
HOXA5	−1,324	Y	0.000008	2.03	1.74	Early pattern	Increasing trend
IGFBP3	−423	Y	0.014216	2.43	1.1	Progression pattern	Increasing trend
IL12A	287	Y	0.043644	2.12	1.06	Cancer-specific pattern	Increasing trend
ITPR3	−1,112	Y	0.033644	4.47	1.02	Cancer-specific pattern	Increasing trend
MMP14	−13	Y	0.024681	2.24	2.78	Early pattern	Increasing trend
NPR2	−618	Y	0.010113	3.55	2.5	Progression pattern	Increasing trend
NTRK2	−656	Y	0.026603	2.31	1.12	Progression pattern	Increasing trend
PITX2	24	Y	0.005856	3.01	1.74	Progression pattern	Increasing trend
POMC	−53	Y	0.043388	4.97	1.14	Progression pattern	Increasing trend
POMC	−400	Y	0.021011	4.97	1.14	Progression pattern	Increasing trend
ROR1	−6	Y	0.025114	8.36	1.38	Progression pattern	Increasing trend

Symbol	Distance (bp) to transcription start site	CpG island in gene promoter region	*Q*-value	Gao cancer (R/G)	Gao adjacent (R/G)	Gao pattern	Illumina analysis
TFAP2C	260	Y	0.000373	4.59	1.32	Progression pattern	Increasing trend
TFPI2	141	Y	0.048975	3.47	0.97	Cancer-specific pattern	Increasing trend
CD34	−339	N	0.017141	4.78	1.06	Cancer-specific pattern	Decreasing trend
CD34	−780	N	0.002913	4.78	1.06	Cancer-specific pattern	Decreasing trend
IRAK3	−185	Y	0.02818	4.12	1.07	Cancer-specific pattern	Decreasing trend
MMP14	−208	N	0.047528	2.24	2.78	Early pattern	Decreasing trend
TMEFF2	−210	Y	0.031635	2.51	1.05	Cancer-specific pattern	Decreasing trend
TNFRSF10C	−7	Y	0.010233	2.58	0.96	Cancer-specific pattern	Decreasing trend